CrossMark

Porous Materials Modified with Fe$_3$O$_4$ Nanoparticles for Arsenic Removal in Drinking Water

Allen Puente-Urbina · Virginia Montero-Campos

Abstract The contamination of drinking water with arsenic has been a problem in a lot of countries around the world because of its toxicological and carcinogenic effects on human health. Porous materials modified with Fe$_3$O$_4$ nanoparticles (Fe$_3$O$_4$ NPs) represent convenient removers for that contaminant. A co-precipitation method of Fe(III) and Fe(II) in alkaline media was applied to obtain Fe$_3$O$_4$ NPs. In a first stage, single nanoparticles were synthesized and stabilized with carboxylic acids. A characterization with attenuated total reflectance Fourier transform infrared spectroscopy (ATR-FTIR), Raman spectroscopy, and X-ray diffraction (XRD) confirms a magnetite-type structure. Moreover, transmission electron microscopy (TEM) and calculations from XRD data using Scherrer's equation indicate an average particle size of 13 nm and an average crystallite size of 10 nm, both independent of the stabilizer used. Then, the co-precipitation method studied was applied to modify kaolin, bentonite, diatomite, and silica and thus prepare magnetic composites having support-magnetite weight ratios of 2:1. Among them, silica-modified material presented the best hydraulic characteristics, an important aspect for large-scale applications such as removal under gravity. This composite has the capacity to remove up to 80 and 70% for initial concentrations of 25 and 50 μg/L, respectively, representing a convenient remover for processes developed in subsequent stages or in continuous flow.

1 Introduction

One of the great challenges of society is to have access to water that can be easily treated for human consumption. Contamination with heavy metals (e.g., lead, cadmium, chromium, mercury, and arsenic) is a major concern because of the effects they can have on human health (Montero-Campos et al. 2010; Lata and Samadder 2016). One of the most worrying cases is arsenic, which can be present in water due to different causes, including natural (e.g., weathering, stone and soil erosion, volcanic emissions) or anthropogenic (e.g., mining wastes, petroleum refining, sewage sludge, agricultural chemicals, ceramic manufacturing industries, incineration of municipal and industrial wastes, and coal fly ash) (Lata and Samadder 2016; Ahoulé et al. 2015). Its main forms are arsenates, sulfides, and sulfosalts and, in lower proportion, arsenide, arsenite, oxides, silicates, and elemental arsenic (Viraraghavan et al. 1999; Onishi 1969). In drinking water, arsenic is available mostly as arsenate and arsenite (i.e., inorganic form) or as methyl and dimethyl arsenic compounds mainly in surface waters (i.e., organic form) (Smedley and Kinniburg 2002).

A. Puente-Urbina (✉) · V. Montero-Campos
Centro de Investigación y de Servicios Químicos y Microbiológicos (CEQIATEC), Escuela de Química, Instituto Tecnológico de Costa Rica, 159-7050, Cartago 30101, Costa Rica
e-mail: apuente@itcr.ac.cr

🐾 Springer

The toxicity of arsenic in water depends on aspects such as its oxidation state (i.e., 3+ or 5+), chemical structure, and solubility in the biological environment. Due to lack of instrumental techniques, the total concentration of As was initially considered as the indicator of toxicity. Subsequently, arsenite (AsO_3^{3-}) was found to be more toxic than arsenate (AsO_4^{3-}). After the development of hyphenated techniques, the existence of methylated As compounds was reported and methylation was considered the detoxification process in humans. Moreover, toxicological studies reported that mono- and dimethylated pentavalent As compounds were less toxic than arsenite [As(III)] (Mandal 2014).

Chronic oral exposure to elevated levels of inorganic arsenic has been linked to gastrointestinal effects, anemia, peripheral neuropathy, skin lesions (hyperpigmentation mainly), and liver or kidney damage in human beings. In addition, long-term exposure to arsenic in water (even at low concentrations) can increase the risk of developing certain types of cancer, including skin, bladder, kidney, and stomach cancer, as well as epigenetic DNA modification and induction of telomere instability (Maiti 2014). The estimated risk of arsenic-induced cancer could be as high as 1 in 100 people for maximum levels of contamination of 50 μg As/L in drinking water. For this reason, the maximum levels of arsenic in drinking water permitted should not be exceeded by 10 μg/L (Schwarzenbach et al. 2010). On the other hand, in addition to water intake, there are other less important ways in which human beings may be exposed to arsenic, such as consumption of food containing significant concentrations or by inhalation (Lata and Samadder 2016; Ahoulé et al. 2015; Castro de Esparza 2008).

The presence of arsenic in water sources has been an issue in several locations worldwide. In Latin America, at least four million people drink water containing levels of arsenic that have risk to their health. In Central America, high As concentrations in volcanic surface and underground waters in the Pacific coast have been detected (Mora-Alvarado 2013; Castro de Esparza 2008). In the specific case of Costa Rica, even with a high coverage of drinking water supply (i.e., 91.2% of the population, according to the last *Report on the State of Nation in Sustainable Human Development* (Herrera 2016)), close to 40,000 people have been exposed to arsenic in water at levels up to 187 μg/L over the last years, far above the value permitted by the local legislation (10 μg/L) (Angulo-Zamora 2015; Mora-Alvarado

2014; Astorga 2013). This led to the declaration of Health Emergency in 2012, whereby the corresponding authorities implemented measures to solve the problem in the short term, including elimination of contaminated wells, interconnection and integration of aqueducts, opening of new wells and aqueducts, implementation of arsenic removal systems including filtration equipments in aqueducts and Kanchan household filters, as well as delivery of water by means of tanker trucks (Angulo-Zamora 2015; Astorga 2013; Astorga and Angulo 2013). Recent advances have been presented in the implementation of treatment plants (Herrera 2016; Angulo-Zamora 2015). Despite all this, long-term solutions are still required for the communities affected.

Several methods are available to treat water containing arsenic, including oxidation, coagulation-flocculation, co-precipitation, adsorption, ion exchange, and membrane implementation (Rojas-Chaves et al. 2015; Romero et al. 2014; Choong et al. 2007; Kartinen and Martin 1995; Cumbal et al. 2014; Elcik et al. 2013; Brandhuber and Amy 2001). A promising method is the application of modified porous materials. These materials take advantage of characteristics of porous supports (e.g., minerals, clays, zeolites, oxides, etc.) such as high porosity, high absorption capacity, and low reactivity in water which make them suitable for several purposes (including water treatment), in addition to the capacity to be modified to improve their arsenic removal capability and the fact that some of them are low-cost raw materials (Montero-Campos and Puente-Urbina 2016; Oliveira et al. 2003; Oliveira et al. 2004; Puente-Urbina et al. 2016).

The use of iron oxides has attracted attention over the last years. Iron oxides have been implemented either individually or with some functionalization, as well as in various matrices, such as the mentioned porous materials and organic materials (e.g., biomass, chitosan, and charcoals) (Starbird-Pérez and Montero-Campos 2015; Saiz et al. 2014; Gao et al. 2011; Thirunavukkarasu et al. 2003; Devi et al. 2014; Wang et al. 2016; Mishra and Mahato 2016; Akin et al. 2012; Baig et al. 2014; Hu et al. 2015; Wang et al. 2014; Qin et al. 2016; Chen et al. 2016). If these are nano-sized oxides, they offer additional advantages such as small volume, high surface area, high reactivity, a large amount of available active sites as well as low diffusion resistance that increases the significance of the application of nanoparticles as adsorbent. In addition, many iron oxides exhibit important magnetic properties that facilitate their containment in

the filtration system using external magnetic fields, or their separation in case of undesired release of the material into the water being processed (Yavuz et al. 2006; Ngomsik et al. 2005; Salem Attia et al. 2013).

In this paper, we present the synthesis of composites obtained from modification of porous materials with magnetite nanoparticles, the characterization of the NPs and the composites using spectroscopic, diffractometric, and microscopic techniques, as well as their study for arsenic removal in drinking water. The aim of this work is to study a magnetic composite with the capacity to remove arsenic from drinking water and with proper hydraulic characteristics for further large-scale applications such as removal under gravity.

2 Experimental

2.1 Materials

Iron(II) chloride tetrahydrate and iron(III) chloride hexahydrate dissolved in deionized water were used as precursors. Concentrated ammonium hydroxide (equivalent to 28.0% w/w NH_3 in water) was used as precipitating agent. Lauric, stearic, and oleic acid dissolved in methanol were used for the stabilization of the single Fe_3O_4 nanoparticles (i.e., Fe_3O_4 nanoparticles not supported in porous materials). All reagents previously mentioned were reagent grade and used without further purification. The porous materials kaolin, bentonite, and silica were all purchased in a purified form, whereas diatomite was obtained as a raw mineral from the company Industrias Mineras S.A. (Barranca, Puntarenas, Costa Rica). All the porous materials were used as received.

2.2 Sample Preparation

2.2.1 Synthesis of Single Fe_3O_4 Nanoparticles (Fe_3O_4 NPs) Stabilized with Carboxylic Acids

Single Fe_3O_4 NPs were synthesized using co-precipitation of Fe(II) and Fe(III) with NH_4OH(aq.) under N_2(g) atmosphere at room temperature, using a procedure similar to the one proposed by Petcharoen and Sirivat (2012), with some modifications. In a typical procedure, 1.5 g of $FeCl_2 \cdot 4H_2O$ and 3.0 g of $FeCl_3 \cdot 6H_2O$ were dissolved in deionized water. Using vigorous stirring, 10 mL of

concentrated NH_4OH(aq.) was added drop by drop. The solution was stirred for 35 min and then centrifuged. The solid obtained (Fe_3O_4 nanoparticles) was washed copiously with water and then methanol to remove the excess of NH_4OH(aq.) and then dispersed in 50 mL of a solution 17 mM of a carboxylic acid (i.e., oleic acid, stearic acid, or lauric acid) in methanol. The mixture was stirred for 3 h and then washed with methanol to remove the excess of carboxylic acid. The product (Fe_3O_4 nanoparticles stabilized with carboxylic acids) was recovered by centrifugation and then dried at 75 °C. The resulting materials are named $Fe_3O_4\_Lauric\ acid$, $Fe_3O_4\_Stearic\ acid$, and $Fe_3O_4\_Oleic\ acid$ for the NPs stabilized with lauric acid, stearic acid, and oleic acid, respectively.

2.2.2 Synthesis of Porous Materials Modified with Fe_3O_4 Nanoparticles

All the syntheses were carried out under N_2(g) atmosphere at room temperature, following a method similar to the one presented for single Fe_3O_4 nanoparticles with some modifications. Magnetic composites were synthesized using co-precipitation of Fe(II) and Fe(III) with NH_4OH(aq.) in a suspension containing the corresponding porous material (i.e., kaolin, bentonite, diatomite, and silica). In a typical procedure, the porous material was dispersed in a solution containing Fe(II) and Fe(III) cations under inert atmosphere. After that, Fe_3O_4 nanoparticles were deposited over the porous substrate using concentrated NH_4OH(aq.) (equivalent to 28.0% w/w NH_3 in water) as precipitating agent. The resulting material was washed with water until neutral pH and then dried. The composite obtained had a support-magnetite mass ratio of 2:1. The products are named $Fe_3O_4@Kaolin$, $Fe_3O_4@Bentonite$, $Fe_3O_4@Diatomite$, and $Fe_3O_4@SiO_2$ for the materials having the porous supports kaolin, bentonite, diatomite and silica, respectively.

2.3 Characterization

2.3.1 ATR-FTIR

ATR-FTIR measurements were developed using a Thermo Scientific Nicolet 380 FT-IR spectrometer with Smart iTR ATR sampling accessory. All the spectra were obtained using 128 scans (both for the sample and the background) and a resolution of 0.482 cm^{-1}.

2.3.2 Raman Spectroscopy Measurements

Raman spectra were recorded using a Thermo Scientific DXR Raman Microscope using a 532-nm laser. For single NPs, data were collected using an exposure time of 10.00 s and 10 exposures (both for the sample and the background). For composites, measurements were developed using an exposure time of 7.00 s and 30 exposures (both for the sample and the background).

2.3.3 XRD

XRD data of single Fe_3O_4 nanoparticles and magnetic composites were acquired with a PANalytical Empyrean diffractometer with $Cok\alpha1$ radiation. Each pattern was obtained in the 2θ range of $15.0091–84.9881°$ with steps of $0.0130°$. The scan step times were 13.7700 s for the single Fe_3O_4 nanoparticle sample and 37.9950 s for the magnetic composites. The obtained data were used to obtain crystallite sizes using Scherrer's equation.

2.3.4 TEM

TEM micrographs were obtained for the single Fe_3O_4 nanoparticles using a JEOL JEM-2100 microscope with an accelerating voltage of 100 kV.

2.4 As Removal

2.4.1 Preliminary Gravity Filtration Tests

To obtain which magnetic composites presented appropriate characteristics to be used as arsenic removal beads for further large-scale applications such as removal under gravity (e.g., without the need of using an external pump), a Büchner funnel having a fitted filter paper in its bottom was packed with each composite and water was allowed to flow. The best properties were presented by the composite that had silica as porous material (i.e., $Fe_3O_4@SiO_2$), then it was selected for further experiments.

2.4.2 Batch Experiments for As Removal

Batch procedures were developed to determine the efficiency of the magnetic composite $Fe_3O_4@SiO_2$ to remove arsenic from water. The following factors were evaluated: amount of remover (0.10–5.00 g/L), removal time (4–22 h), concentration of arsenic (25–50 μg/L), and pH (5 and > 7). In each run, Erlenmeyer flasks (250 mL)

containing a fixed dosage of $Fe_3O_4@SiO_2$ and the same volume of arsenic solution were placed in a mechanical shaker at constant temperature for a specific time. Then, the mixture was separated under vacuum using a 47-mm magnetic filter funnel with glass fiber filter paper of 0.45 μm of pore size. Total arsenic was determined before and after the removal procedure, using a Perkin Elmer AAnalyst-800 atomic absorption spectrometer with a FIAS-100 hydride generation system. All As measurements were carried out using a method that typically had a detection limit of 0.72 μg/L and a quantification limit of 2.38 μg/L according to Miller and Miller (2010).

3 Results and Discussion

The preparation of composite materials is attractive because it allows taking advantage of different properties of the components involved, improving the functionality of the resulting materials in comparison with their separate parts. In order to remove arsenic from water by filtration, it is desirable for the water to have contact with a large surface of material capable of properly retaining the contaminant. The present research sought this by applying modified porous materials. The chosen porous materials (i.e., bentonite, kaolinite, diatomite, and silica) have desirable properties such as high porosity and surface area, chemical inertness for the intended application, and a significant affinity to water, which favors the contact between the filter medium and the water under treatment. These supports were modified by deposition of nano-sized magnetite particles, in order to obtain composites that allow removal of arsenic from water effectively, taking advantage of the affinity of this type of oxides towards arsenic and their high contact surface. Moreover, the magnetic properties of the NPs allow the confinement of the composite in the filtration system, as well as the retention of particles that could be undesirably released, both using an external magnetic field.

Composite syntheses began with a preliminary study of synthesis of Fe_3O_4 nanoparticles (Fig. 1a). At a later stage, similar conditions were applied but using porous materials in reaction media in order to obtain the functional magnetic composites (Fig. 1b). All the reactions were carried out under simple working conditions that could be easily scaled up later. On the other hand, bentonite, kaolinite, diatomite, and silica represent porous materials which are low cost and easy to acquire.
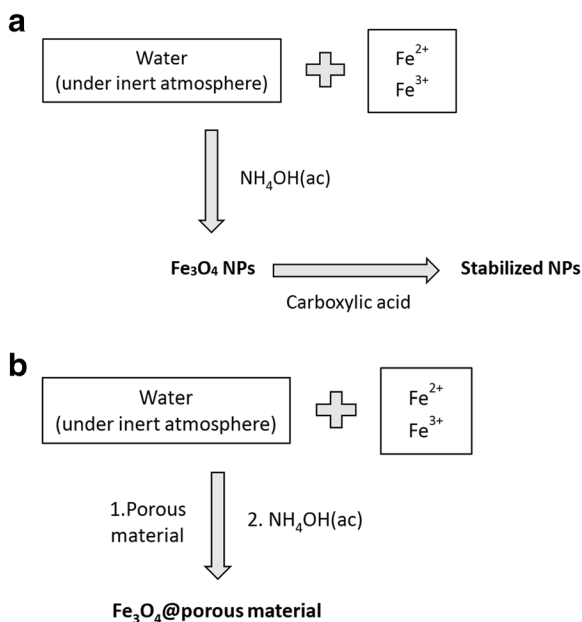
Fig. 1 Schemes of **a** syntheses of single Fe_3O_4 nanoparticles using a co-precipitation method and **b** preparation of magnetic composites using co-precipitation over porous materials

NP syntheses were developed at room temperature from Fe^{2+} and Fe^{3+} in the presence of a base, using water as solvent. On the other hand, bubbling of $N_2(g)$ was used to avoid oxidation and thus maintain an adequate Fe(III):Fe(II) ratio for the preparation of magnetite, and a strong stirring was presented during the complete process. The formation of those NPs in alkaline media can be described as a co-precipitation process in which a dark precipitate appears just after the mixing of a solution containing Fe^{2+} and Fe^{3+} with a basic solution. In general, this process can be depicted as follows (Iida et al. 2007):

$$Fe^{2+} + 2Fe^{3+} + 8OH^- \rightarrow Fe_3O_4 + 4H_2O \qquad (1)$$
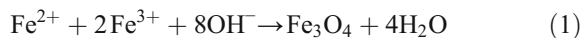
Moreover, Petcharoen and Sirivat (2012) explained in more detail the formation of Fe_3O_4 nanoparticles by the following reactions:

$$Fe^{2+} + 2OH^- \rightarrow Fe(OH)_2 \qquad (2)$$

$$Fe^{3+} + 3OH^- \rightarrow Fe(OH)_3 \qquad (3)$$

$$Fe(OH)_2 + 2Fe(OH)_3 \rightarrow Fe_3O_4 + 4H_2O \qquad (4)$$

This process is affected by reaction conditions that could influence the way in which the precipitate is

formed, including some related to the substances involved, such as type and concentration of the reagents, nature of the solvent and ratio of Fe(III) to Fe(II), and other operative conditions such as temperature, pH, digestion time, stirring rate, presence of light, alkali addition rate, presence of a stabilizer and stage of the process in which it is incorporated, among others (Mascolo et al. 2013; Aphesteguy et al. 2015; Iida et al. 2007; Petcharoen and Sirivat 2012; Gnanaprakash et al. 2007; Valenzuela et al. 2009; Shen et al. 2014; Wan et al. 2007).

The NPs were characterized by different instrumental techniques, including spectroscopic, diffractometric, and microscopic techniques. To study the properties of the products avoiding the risk of agglomeration of the particles, coatings with different carboxylic acids (i.e., lauric, oleic, and stearic acids) were developed. However, bare nanoparticles were also analyzed.

Regarding the spectroscopic analyses of magnetic nanoparticles, the results of the ATR-FTIR are shown in Fig. 2. Measurements developed for bare NPs showed two important signals, one at 3417 cm^{-1} corresponding to the stretching of O–H bonds presented in surface hydroxyl groups as well as adsorbed water molecules, and another at 1600 cm^{-1} due to H–O–H bending in water molecules. On the other hand, stabilized nanoparticles (i.e., nanoparticles coated with carboxylic acids) presented differences in their spectra in comparison with bare NPs because of the presence of the coatings. In this concern, stabilized nanoparticles presented differences in the signal related to O–H bond stretching, but more significant was the appearance of new bands, including two at 2921 and 2852 cm^{-1} that correspond to the symmetric and asymmetric methylene stretching of the coating agents, and two at 1519 and 1428 cm^{-1} due to the presence of symmetric and asymmetric stretching vibrations of carboxyl groups. These last bands suggest the surface modification of the nanoparticles by the carboxylate groups of the carboxylic acids, after the interaction between the hydrated surface of the oxide and the corresponding carboxylic acid. On the other hand, considering the Raman spectroscopy measurements (Fig. 3), a main signal around 668 cm^{-1} appeared. This signal is consistent with previous reports presented in literature for magnetite, and it is attributed to an allowed transition A1g (Shebanova and Lazor 2003; Slavov et al. 2010).

Considering XRD analyses, the measurements for stabilized single Fe_3O_4 nanoparticles (Fig. 4) confirm a
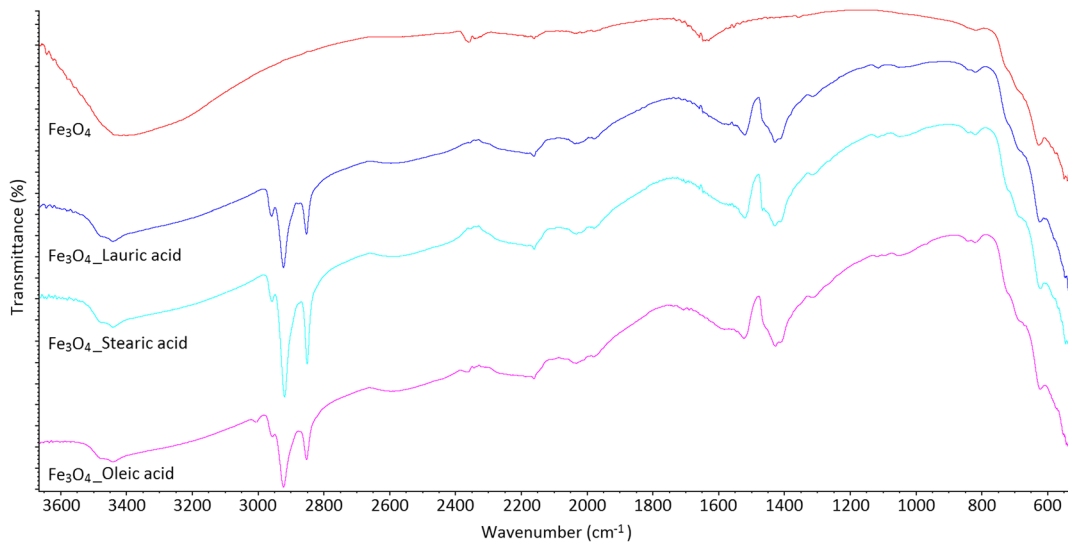
Fig. 2 ATR-FTIR spectra of single Fe_3O_4 nanoparticles

magnetite-type structure. The structure was successfully indexed according to ICDD powder diffraction file number 98-009-8084, with the crystallographic parameters shown in Table 1. Crystallite sizes of the samples were calculated using Scherrer's equation:

$$d = \frac{K\lambda}{\beta \cos\theta} \tag{5}$$

where d is the crystal size, K is the shape factor, λ is the X-ray wavelength, β is the width at half maximum of the strongest peak, and θ is Bragg's angle. Using a K shape

factor of 0.89 for spherical Fe_3O_4 NPs (Cheng et al. 2010) and the other corresponding values related to the XRD measurements, crystallite sizes of 10.7, 10.4, and 10.6 nm for the NPs stabilized with lauric acid, stearic acid, and oleic acid, respectively, were obtained (Table 2).

Magnetite nanoparticles were also analyzed using TEM measurements. The synthesized NPs had spherical morphology as can be seen in Fig. 5 for the stabilized NPs. In addition, the average size of the coated NPs was 12.9 ± 6.8, 13.3 ± 7.0, and 13.5 ± 6.9 nm for the
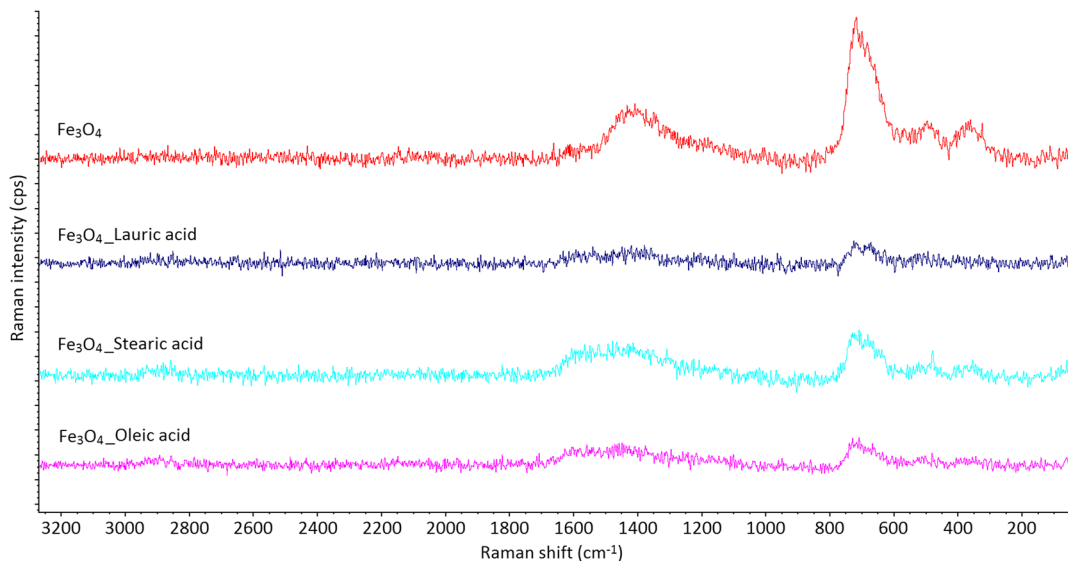

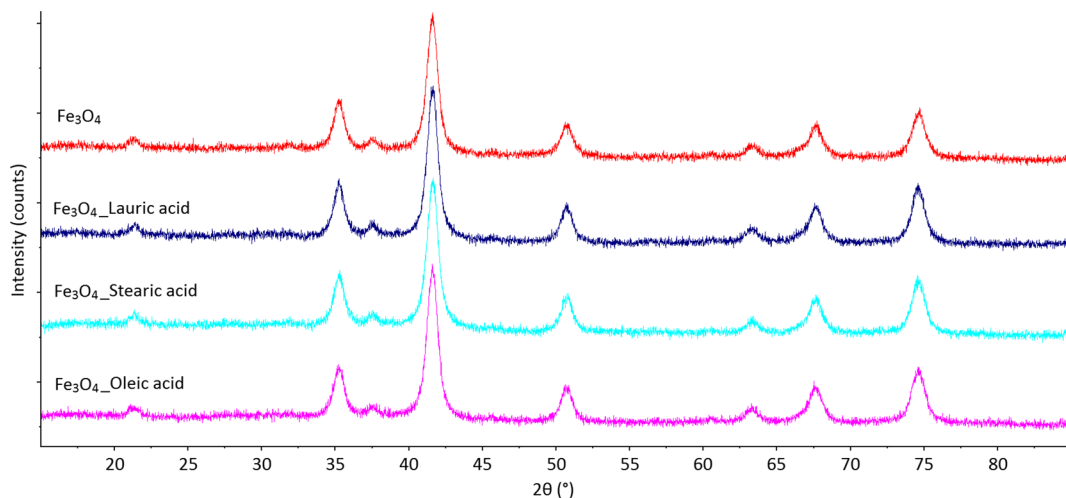**Fig. 3** Raman spectra of single Fe_3O_4 nanoparticles

Fig. 4 XRD patterns of single Fe_3O_4 nanoparticles

stabilizers lauric acid, stearic acid, and oleic acid, respectively. There was no significant difference among these samples, despite the different coatings of the particles. This means that the particle size is determined by the co-precipitation process of Fe(II) and Fe(III), regardless of the coating performed in the subsequent step. The results are consistent with the report of Gnanaprakash et al. (2007), who found that the growth process for magnetite nanocrystals is completed in very short times, considering that coating processes were developed after the preparation of the NPs in which a stirring time of 35 min is involved.

The information presented above allowed laying the foundations for further preparation and characterization of composite materials by modification of bentonite, kaolinite, diatomite, and silica with Fe_3O_4 NPs. The

Table 1 Crystallographic parameters of magnetite 98-009-8084

Crystal system	Monoclinic
Space group	P 1 2/m 1
Space group number	10
a (Å)	5.9420
b (Å)	5.9250
c (Å)	8.3860
Alpha	90.0000
Beta	90.2550
Gamma	90.0000
Calculated density (g/cm^3)	5.21
Volume of cell (10^6 pm^3)	295.24
Z	4.00
RIR	1.55

materials were synthesized using the scheme presented in Fig. 1b. On the other hand, those materials were characterized using Raman spectroscopy and XRD. Raman spectroscopy measurements showed the transition signal A1g mentioned for the individual nanoparticle samples (i.e., not immobilized on porous materials) (Fig. 6). Similarly, XRD patterns coincide with the structure previously mentioned (Fig. 7). Moreover, the crystallite sizes were calculated using Scherrer's equation for those samples whose diffraction patterns did not show overlap of the most intense magnetite signal near $2\theta = 41.6°$ with characteristic signals of the porous supports. This was possible with composite materials whose supports were silica and diatomite, which had crystallite sizes of 10.3 and 9.8 nm, respectively. These results allow corroborating the applicability of the proposed method for the preparation of porous materials modified with magnetite nanoparticles.

Iron oxides have been proved to be effective adsorbers of arsenic (Mamindy-Pajany et al. 2011; Giménez et al. 2007). Surface properties are key factors

Table 2 Crystallite size measured using Scherrer's equation from XRD data and particle size using TEM

Sample	Crystallite size (nm)	Particle size (nm)
Fe_3O_4_Lauric acid	10.7	12.9 ± 6.8
Fe_3O_4_Stearic acid	10.4	13.3 ± 7.0
Fe_3O_4_Oleic acid	10.6	13.5 ± 6.9
Fe_3O_4@SiO_2	10.3	–
Fe_3O_4@Diatomite	9.8	–

Fig. 5 TEM micrographs (**a** Fe$_3$O$_4$ nanoparticles stabilized with lauric acid, **b** Fe$_3$O$_4$ nanoparticles stabilized with stearic acid, **c** Fe$_3$O$_4$ nanoparticles stabilized with oleic acid) and size distribution of single Fe$_3$O$_4$ nanoparticles (**d**)
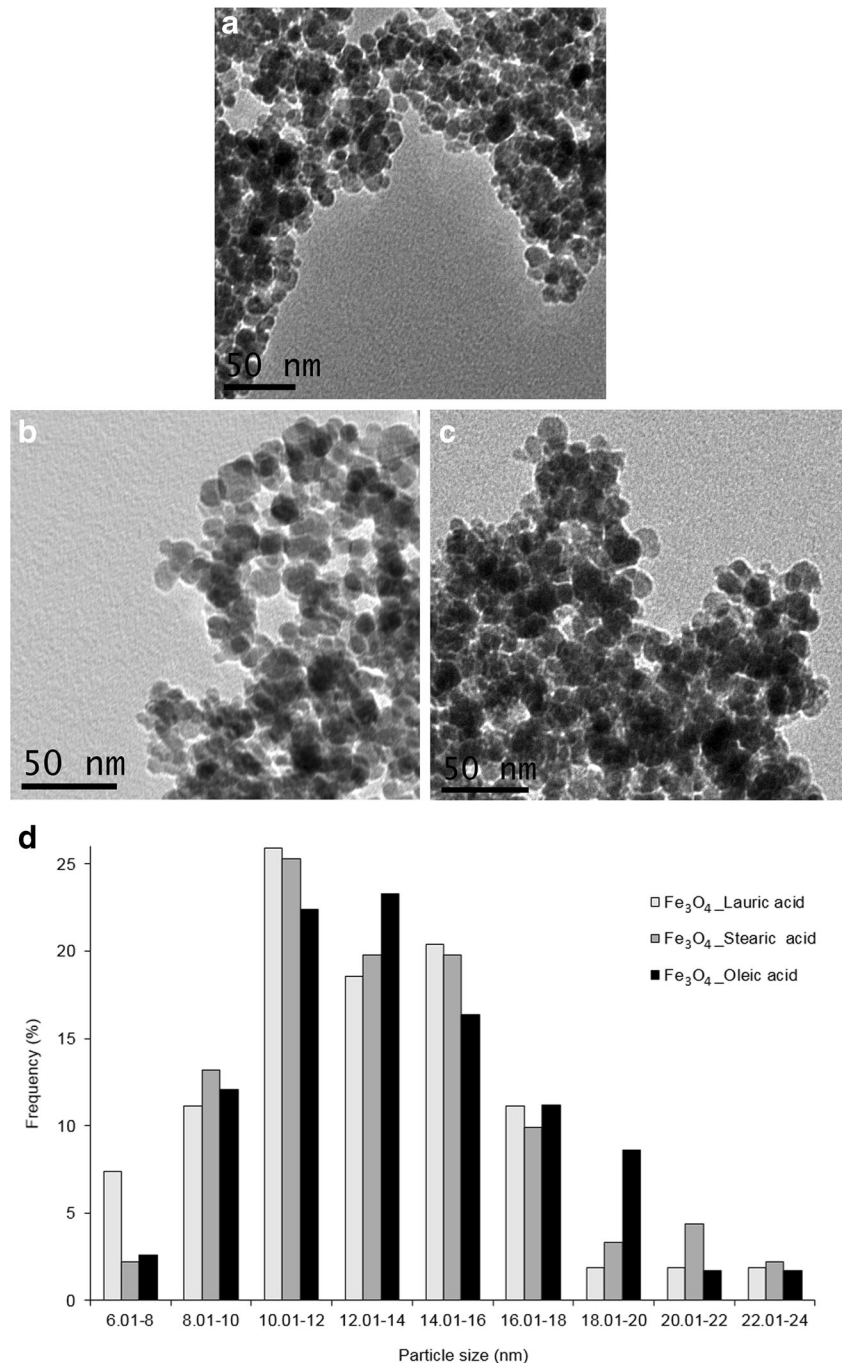
of the performance of those materials because they influence the interaction with arsenic forms (Yean et al. 2005). Other important aspects to be considered are the capacity to present reversible adsorption processes to have reusable materials after regeneration as well as the capacity to be confined and recovered. For these reasons, magnetic nanomaterials have gained great

attention in recent years. Among them, magnetite nanoparticles have enhanced adsorption properties because of their great surface area and the fraction of the atoms that are in the surface, the capacity to remove both arsenate and arsenite, as well as magnetic properties that allow them to be confined using low-field magnets (Shipley et al. 2009;
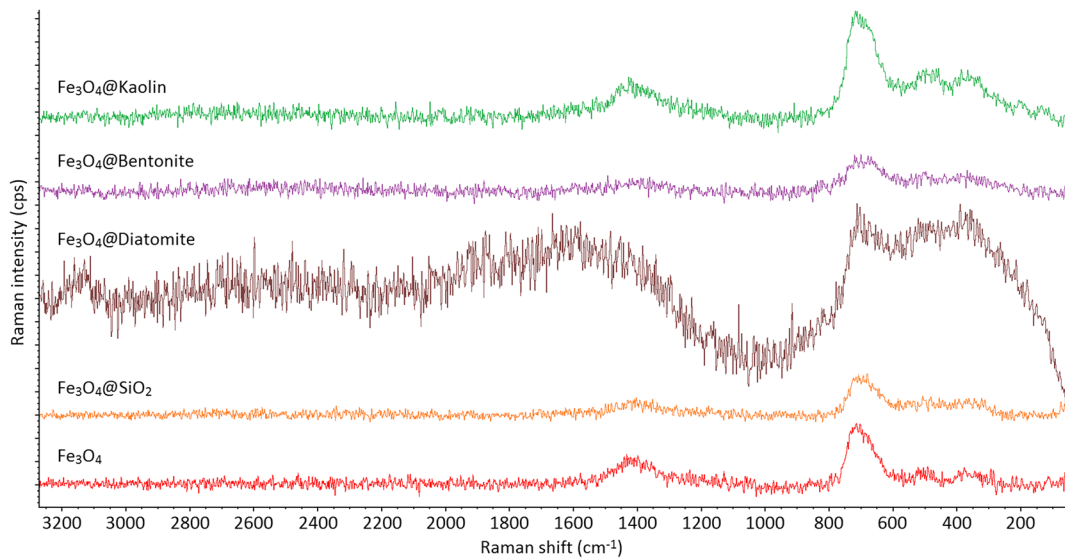
Fig. 6 Raman spectra of magnetic composites

Yavuz et al. 2006; Yean et al. 2005; Mayo et al. 2007).

Considering the application of the composites intended for arsenic removal in water, the experiments started with appropriate filtration tests to evaluate hydraulic performances of the materials prepared. This is particularly relevant for further applications in continuous-flow systems operating by gravity (e.g., without the use of external pumps) in which the composite materials are used as removers of such contaminant (Montero-Campos and Puente-Urbina 2016). The

material that showed the best hydraulic performance was the composite material whose support is silica (i.e., $Fe_3O_4@SiO_2$), therefore the one used in later tests. The experiments were carried out evaluating some variables that could affect the removal process such as pH, removal time, arsenic concentration, and amount of magnetic composite (i.e., the adsorbent). For an initial arsenic concentration of 50 μg/L and a pH > 7, there is a considerable removal increase between 0.10 and 1.00 g of adsorbent per 1 L of arsenic solution, which tends to continue without apparent increase. In the case of
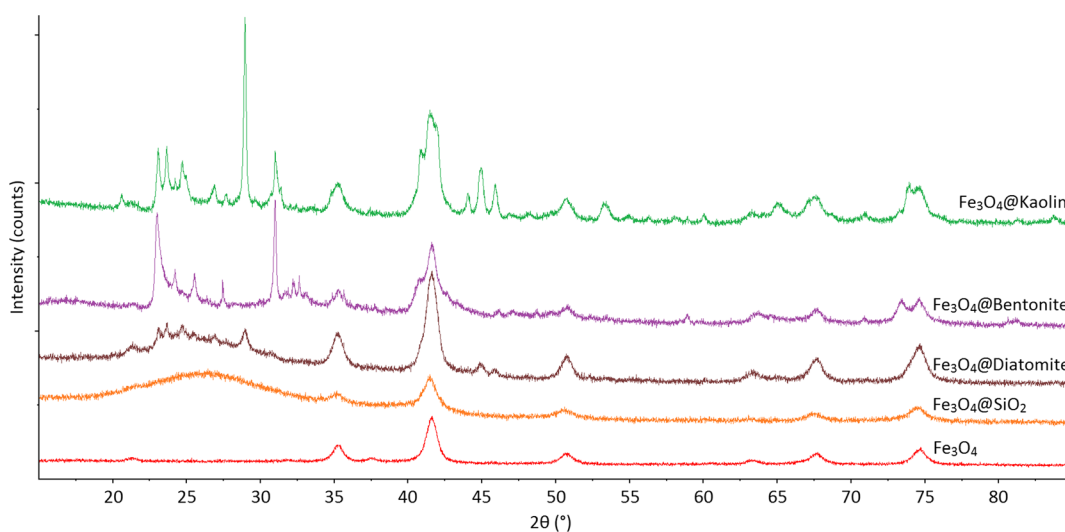

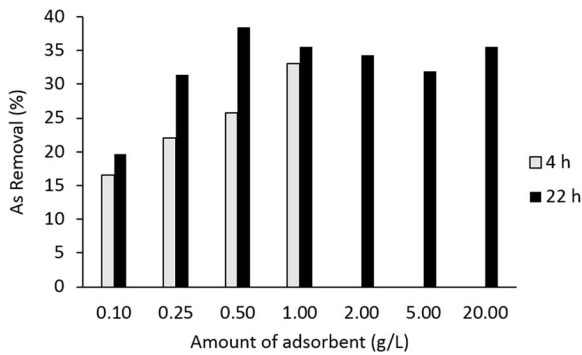**Fig. 7** XRD diffraction patterns of magnetic composites

Fig. 8 Batch arsenic removal using pH > 7 and concentration of 50 μg/L

Fig. 10 Batch arsenic removal using pH = 5 and concentration of 25 μg/L

1.00 g/L, similar percentages of removal for both short times (4 h) and longer times (22 h) were observed (Fig. 8). Removal percentages are significantly improved by decreasing the pH of the initial solution to 5 (Fig. 9), reaching maximum removals of 70%. On the other hand, lower concentrations allowed achieving a removal of up to 60% in 4 h with that pH and up to 80% in 22 h (Fig. 10).

Adsorption tests show clear influences of the variables evaluated. Considering the time tested, the amount of arsenic adsorbed increases as expected for longer contact times among the species involved in the removal processes. A variation with the pH of the initial solutions was also observed. This pH modifies the surface charge. It is reported that the point of zero charge is reached at pH = 6.8 for Fe_3O_4 NPs (Yean et al. 2005), meaning that lower pH values lead to positive surfaces. Such condition affects the interaction between the surface and the arsenic species. In fact, arsenate removal increases with lower pH values for different iron oxides including magnetite (Yean et al. 2005; Raven et al. 1998; Mamindy-Pajany et al. 2011; Giménez et al. 2007),
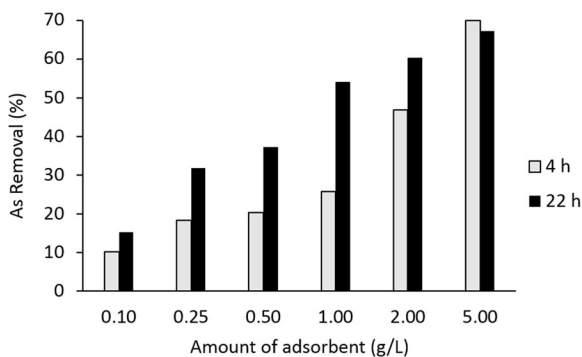

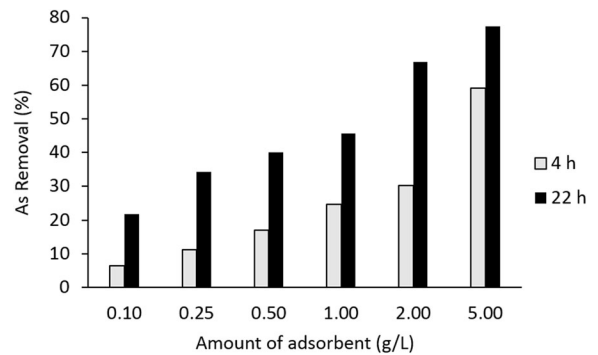**Fig. 9** Batch arsenic removal using pH = 5 and concentration of 50 μg/L

while arsenite has been reported with a different behavior, increasing the removal with increasing pH in some cases (Raven et al. 1998; Jain and Loeppert 2000; Dixit and Hering 2003) or being independent of pH in others (Dixit and Hering 2003; Yean et al. 2005). In our case, an increase in the adsorption with lower pH values suggests the presence of mainly As(V), as expected for testing solutions prepared from commercial standards which are stored under air in acidic media.

Finally, the arsenic removal results showed a higher initial increase at the shorter time evaluated (4 h) for higher concentrations of arsenic. This is reasonable considering that a higher concentration of arsenic ions could affect their initial adsorption rate and, consequently, the percentage of arsenic removed. However, at longer times (22 h), the removal percentage of arsenic decreased with the increase of the initial arsenic concentration. By that time, the system should be closer to equilibrium, meaning that enough time has been provided for the arsenic ions to compete for the available surface active sites (i.e., binding sites). There is a certain capacity of the surface active sites for a given amount of adsorbent, resulting in a lack of sufficient sites for all the arsenic ions presented in the initial solution, resulting in the trend obtained (Salem Attia et al. 2013; Chen et al. 2016; Mamindy-Pajany et al. 2011). Nevertheless, the results suggest that convenient removal of arsenic can be achieved. Treatment could be done in subsequent stages, in which a continuous decrease could be achieved to obtain a certain arsenic concentration. In fact, previous reports have proved that this material is effective to treat water with high contents of arsenic in continuous flow and reach levels lower than those established in the Costa Rican regulation (10 μg/L) (Montero-Campos and Puente-Urbina 2016).

4 Conclusions

A complete study for the preparation and characterization of composite materials for arsenic removal in water is presented. An initial study of the synthesis and characterization of Fe_3O_4 nanoparticles allowed the determination of the properties of the resulting materials as well as the obtainment of a method suitable for further preparation of magnetic composites. Then, composite materials obtained by the co-precipitation of Fe(III) and Fe(III) in alkaline media over kaolinite, bentonite, diatomite, and silica were prepared. Among them, modified silica presented the best hydraulic properties that allow its consideration for further applications in continuous-flow systems operating by gravity. This material was able to remove properly arsenic from waters of 50 µg/L and 25 mg/L, being affected by the initial As concentration, amount of adsorbent, removal time, and pH.

References

Ahoulé, D. G., Lalanne, F., Mendret, J., Brosillon, S., & Maïga, A. H. (2015). Arsenic in African waters: a review. *Water, Air, and Soil Pollution*. doi:10.1007/s11270-015-2558-4.

Akin, I., Arslan, G., Tor, A., Ersoz, M., & Cengeloglu, Y. (2012). Arsenic(V) removal from underground water by magnetic nanoparticles synthesized from waste red mud. *Journal of Hazardous Materials*. doi:10.1016/j.jhazmat.2012.06.024.

Angulo-Zamora, F. (2015). Vigesimoprimer Informe Estado de la Nación en Desarrollo Humano Sostenible: Informe final, Gestión del Recurso Hídrico y Saneamiento en Costa Rica. Programa Estado de la Nación. http://estadonacion.or.cr/files/biblioteca_virtual/021/ambiente/Angulo_RH_y_saneamiento.pdf.

Aphesteguy, J. C., Kurlyandskaya, G. V., De Celis, J. P., Safronov, A. P., & Schegoleva, N. N. (2015). Magnetite nanoparticles prepared by co-precipitation method in different conditions.

Materials Chemistry and Physics. doi:10.1016/j.matchemphys.2015.05.044.

Astorga, Y. (2013). Decimonoveno Informe Estado de la Nación en Desarrollo Humano Sostenible: Informe final, Gestión del Recurso Hídrico. Programa Estado de la Nación. http://estadonacion.or.cr/files/biblioteca_virtual/019/astorga_2013.pdf.

Astorga, Y. & Angulo, F. (2013). Vigésimo Informe Estado de la Nación en Desarrollo Humano Sostenible: Informe final, Gestión del Recurso Hídrico y Saneamiento. Programa Estado de la Nación. http://estadonacion.or.cr/files/biblioteca_virtual/020/ambiente/Astorga%20y%20Angulo_Recurso%20H%C3%ADdrico%20y%20Saneamiento.pdf.

Baig, S. A., Sheng, T., Sun, C., Xue, X., Tan, L., & Xu, X. (2014). Arsenic removal from aqueous solutions using Fe_3O_4-HBC composite: effect of calcination on adsorbents performance. *PloS One, 9*(6), e100704. doi:10.1371/journal.pone.0100704.

Brandhuber, P., & Amy, G. (2001). Arsenic removal by a charged ultrafiltration membrane—influences of membrane operating conditions and water quality on arsenic rejection. *Desalination*. doi:10.1016/S0011-9164(01)00350-2.

Castro de Esparza, M. L. (2008). The presence of arsenic in drinking water in Latin America and its effect on public health. In: J. Bundschuh, M. A. Armienta, P. Birkle, P. Bhattacharya, J. Matschullat, & A. B. Mukherjee (Ed.), *Natural arsenic in groundwaters of Latin America*. Boca Raton: CRC Press.

Chen, H., Liu, L., Gong, R., Wei, R., Yi, Q., & Qiu, A. (2016). Comparison of kinetics of arsenic(V) adsorption on two types of red soil weathered from granite and sandstone. *Water, Air, & Soil Pollution*. doi:10.1007/s11270-016-3107-5.

Cheng, Y., Tan, R., Wang, W., Guo, Y., Cui, P., & Song, W. (2010). Controllable synthesis and magnetic properties of Fe_3O_4 and $Fe_3O_4@SiO_2$ microspheres. *Journal of Materials Science*. doi:10.1007/s10853-010-4583-4.

Choong, T. S. Y., Chuah, T. G., Robiah, Y., Gregory Koay, F. L., & Azni, I. (2007). Arsenic toxicity, health hazards and removal techniques from water: an overview. *Desalination*. doi:10.1016/j.desal.2007.01.015.

Cumbal, L., German, M., Sengupta, A., & Shengheng, H. (2014). Robust and reusable hybrid nanosorbent to mitigate arsenic crisis: from laboratory to masses in the field. In: M. I. Litter, H. B. Nicolli, M. Meichtry, N. Quici, J. Bundschuh, P. Bhattacharya, & R. Naidu (Ed.), *One century of the discovery of arsenicosis in Latin America (1914–2014)* (pp. 797–801). Boca Raton: CRC Press.

Devi, R. R., Umlong, I. M., Das, B., Borah, K., Thakur, A. J., Raul, P. K., Banerjee, S., & Singh, L. (2014). Removal of iron and arsenic (III) from drinking water using iron oxide-coated sand and limestone. *Applied Water Science*. doi:10.1007/s13201-013-0139-5.

Dixit, S., & Hering, J. (2003). Comparison of arsenic (V) and arsenic (III) sorption onto iron oxide minerals: implications for arsenic mobility. *Environmental Science & Technology*. doi:10.1021/es030309t.

Elcik, H., Cakmakci, M., Sahinkaya, E., & Ozkaya, B. (2013). Arsenic removal from drinking water using low pressure membranes. *Industrial & Engineering Chemistry Research*. doi:10.1021/ie401393p.

Gao, M., Li, W., Dong, J., Zhang, Z., & Yang, B. (2011). Synthesis and characterization of superparamagnetic $Fe_3O_4@SiO_2$ core-shell composite nanoparticles. *World Journal of Condensed Matter Physics*. doi:10.4236/wjcmp.2011.12008.

Giménez, J., Martínez, M., de Pablo, J., Rovira, M., & Duro, L. (2007). Arsenic sorption onto natural hematite, magnetite, and goethite. *Journal of Hazardous Materials*. doi:10.1016/j.jhazmat.2006.07.020.

Gnanaprakash, G., Philip, J., Jayakumar, T., & Raj, B. (2007). Effect of digestion time and alkali addition rate on physical properties of magnetite nanoparticles. *Journal of Physical Chemistry B*. doi:10.1021/jp071299b.

Herrera, J. (2016). Vigesimosegundo Informe Estado de la Nación en Desarrollo Humano Sostenible: Informe final, Recurso Hídrico y Saneamiento: Avances y Desafíos. Programa Estado de la Nación. http://estadonacion.or.cr/files/biblioteca_virtual/022/Ambiente/Herrera_J_2016 Recursos_hidricos.pdf.

Hu, X., Ding, Z., Zimmerman, A. R., Wang, S., & Gao, B. (2015). Batch and column sorption of arsenic onto iron-impregnated biochar synthesized through hydrolysis. *Water Research*. doi:10.1016/j.watres.2014.10.009.

Iida, H., Takayanagi, K., Nakanishi, T., & Osaka, T. (2007). Synthesis of Fe_3O_4 nanoparticles with various sizes and magnetic properties by controlled hydrolysis. *Journal of Colloid and Interface Science*. doi:10.1016/j.jcis.2007.05.047.

Jain, A., & Loeppert, R. H. (2000). Effect of competing anions on the adsorption of arsenate and arsenite by ferrihydrite. *Journal of Environmental Quality*. doi:10.2134/jeq2000.00472425002900050008x.

Kartinen, E. O., & Martin, C. J. (1995). An overview of arsenic removal processes. *Desalination*. doi:10.1016/j.desal.2004.07.031.

Lata, S., & Samadder, S. R. (2016). Removal of arsenic from water using nano adsorbents and challenges: a review. *Journal of Environmental Management*. doi:10.1016/j.jenvman.2015.10.039.

Maiti, S. (2014). Arsenic-induced mutagenesis and carcinogenesis: a possible mechanism. In S. J. S. Flora (Ed.), *Handbook of arsenic toxicology* (pp. 233–279). Cambridge: Academic Press.

Mamindy-Pajany, Y., Hurel, C., Marmier, N., & Roméo, M. (2011). Arsenic (V) adsorption from aqueous solution onto goethite, hematite, magnetite and zero-valent iron: effects of pH, concentration and reversibility. *Desalination*. doi:10.1016/j.desal.2011.07.046.

Mandal, B. K. (2014). Changing concept of arsenic toxicity with development of speciation techniques. In S. J. S. Flora (Ed.), *Handbook of arsenic toxicology* (pp. 179–201). Cambridge: Academic Press.

Mascolo, M. C., Pei, Y., & Ring, T. A. (2013). Room temperature co-precipitation synthesis of magnetite nanoparticles in a large ph window with different bases. *Materials*. doi:10.3390/ma6125549.

Mayo, J. T., Yavuz, C., Yean, S., Cong, L., Shipley, H., Yu, W., Falkner, J., Kan, A., Tomson, M., & Colvin, V. L. (2007). The effect of nanocrystalline magnetite size on arsenic removal. *Science and Technology of Advanced Materials*. doi:10.1016/j.stam.2006.10.005.

Miller, J. N., & Miller, J. C. (2010) Statistics and chemometrics for analytical chemistry, 6th ed. (pp. 124–126). London: Pearson.

Mishra, T., & Mahato, D. K. (2016). A comparative study on enhanced arsenic(V) and arsenic(III) removal by iron oxide and manganese oxide pillared clays from ground water. *Journal of Environmental Chemical Engineering*. doi:10.1016/j.jece.2016.01.022.

Montero-Campos, V., & Puente-Urbina, A. (2016). Continuous-flow removal of arsenic in drinking water by filtering down through $Fe_3O_4@SiO_2$ magnetic composite. *Journal of Water Resource and Protection*. doi:10.4236/jwarp.2016.85051.

Montero-Campos, V., Quesada-Kimsey, J., Ledezma-Espinoza, A., & Sandoval-Mora, J. (2010). Determinación de arsénico en abastecimientos de agua para consumo humano de la provincia de Cartago, Costa Rica. *Acta Médica Costarricense, 52*(2), 96–101.

Mora-Alvarado, D. A. (2013). Agua para consumo humano: Estudio comparativo de la contaminación por arsénico en Argentina, Chile y los países de Centroamerica. Tres Ríos: Acueductos y Alcantarillados.

Mora-Alvarado, D. A. (2014). La problemática del arsénico: Costa Rica en el contexto Latinoamericano. Acueductos y Alcantarillados. Tres Ríos: Acueductos y Alcantarillados.

Ngomsik, A. F., Bee, A., Draye, M., Cote, G., & Cabuil, V. (2005). Magnetic nano- and microparticles for metal removal and environmental applications: a review. *Comptes Rendus Chimie*. doi:10.1016/j.crci.2005.01.001.

Oliveira, L. C. A., Rios, R. V. R. A., Fabris, J. D., Sapag, K., Garg, V. K., & Lago, R. M. (2003). Clay-iron oxide magnetic composites for the adsorption of contaminants in water. *Applied Clay Science*. doi:10.1016/S0169-1317(02)00156-4.

Oliveira, L. C., Petkowicz, D. I., Smaniotto, A., & Pergher, S. B. C. (2004). Magnetic zeolites: a new adsorbent for removal of metallic contaminants from water. *Water Research*. doi:10.1016/j.watres.2004.06.008.

Onishi, H. (1969). Arsenic. In K. H. Wedepohl (Ed.), *Handbook of geochemistry (chapter 33)*. New York: Springer-Verlag.

Petcharoen, K., & Sirivat, A. (2012). Synthesis and characterization of magnetite nanoparticles via the chemical co-precipitation method. *Materials Science and Engineering: B*. doi:10.1016/j.mseb.2012.01.003.

Puente-Urbina, A., Hollenbach, J., Céspedes-Camacho, I. F., Matysik, J., & Valle-Bourrouet, G. (2016). Effect of pretreatment temperature on the surface modification of diatomite with trimethylchlorosilane. *Journal of Porous Materials*. doi:10.1007/s10934-016-0204-1.

Qin, C., Liu, L., Han, Y., & Chen, C. (2016). Mesoporous magnetic ferrum-yttrium binary oxide: a novel adsorbent for efficient arsenic removal from aqueous solution. *Water, Air, & Soil Pollution*. doi:10.1007/s11270-016-3032-7.

Raven, K. P., Jain, A., & Loeppert, R. H. (1998). Arsenite and arsenate adsorption on ferrihydite: kinetics, equilibrium, and adsorption envelopes. *Environmental Science and Technology*. doi:10.1021/es970421p.

Rojas-Chaves, P., Vargas-Benavides, M. J., Araya-Obando, A., Valverde-Cerdas, J., & Romero-Esquivel, L. G. (2015). Estudio de remoción de arsénico en agua potable a nivel domiciliar mediante oxidación solar y coagulación-floculación. *Tecnología en Marcha*. doi:10.18845/tm.v28i4.2443.

Romero, L. G., Valverde, J., Rojas, P., Vargas, MJ, & Araya, J. A. (2014). Exploring low-cost arsenic removal alternatives in Costa Rica. In: M. I. Litter, H. B. Nicolli, M. Meichtry, N. Quici, J. Bundschuh, P. Bhattacharya, & R. Naidu (Ed.), *One century of the discovery of arsenicosis in Latin America (1914–2014)* 853–855. Boca Raton: CRC Press.

Saiz, J., Bringas, E., & Ortiz, I. (2014). Functionalized magnetic nanoparticles as new adsorption materials for arsenic removal from polluted waters. *Journal of Chemical Technology & Biotechnology.* doi:10.1002/jctb.4331.

Salem Attia, T. M., Hu, X. L., & Yin, D. Q. (2013). Synthesized magnetic nanoparticles coated zeolite for the adsorption of pharmaceutical compounds from aqueous solution using batch and column studies. *Journal of Experimental Nanoscience.* doi:10.1016/j.chemosphere.2013.07.046.

Schwarzenbach, R. P., Egli, T., Hofstetter, T. B., von Gunten, U., & Wehrli, B. (2010). Global water pollution and human health. *Annual Review of Environment and Resources.* doi:10.1146/annurev-environ-100809-125342.

Shebanova, O. N., & Lazor, P. (2003). Raman spectroscopic study of magnetite ($FeFe_2O_4$): a new assignment for the vibrational spectrum. *Journal of Solid State Chemistry.* doi:10.1016/S0022-4596(03)00294-9.

Shen, L., Qiao, Y., Guo, Y., Meng, S., Yang, G., Wu, M., & Zhao, J. (2014). Facile co-precipitation synthesis of shape-controlled magnetite nanoparticles. *Ceramics International.* doi:10.1016/j.ceramint.2013.07.037.

Shipley, H. J., Yean, S., Kan, A. T., & Tomson, M. B. (2009). Adsorption of arsenic to magnetite nanoparticles: effect of particle concentration, pH, ionic strength, and temperature. *Environmental Toxicology and Chemistry.* doi:10.1897/08-155.1.

Slavov, L., Abrashev, M. V., Merodiiska, T., Gelev, C., Vandenberghe, R. E., Markova-Deneva, I., & Nedkov, I. (2010). Raman spectroscopy investigation of magnetite nanoparticles in ferrofluids. *Journal of Magnetism and Magnetic Materials.* doi:10.1016/j.jmmm.2010.01.005.

Smedley, P. L., & Kinniburg, D. G. (2002). A review of the source, behaviour and distribution of arsenic in natural waters. *Applied Geochemistry.* doi:10.1016/S0883-2927(02)00018-5.

Starbird-Pérez, R., & Montero-Campos, V. (2015). Synthesis of magnetic iron oxide nanoparticles toward arsenic removal from drinking water. *Tecnología en Marcha.* doi:10.18845/tm.v28i3.2410.

Thirunavukkarasu, O. S., Viraraghavan, T., & Subramanian, K. S. (2003). Arsenic removal from drinking water using iron oxide-coated sand. *Water, Air, & Soil Pollution.* doi:10.1023/A:1022073721853.

Valenzuela, R., Fuentes, M. C., Parra, C., Baeza, J., Duran, N., Sharma, S. K., Knobel, M., & Freer, J. (2009). Influence of stirring velocity on the synthesis of magnetite nanoparticles (Fe_3O_4) by the co-precipitation method. *Journal of Alloys and Compounds.* doi:10.1016/j.jallcom.2009.08.087.

Viraraghavan, T., Subramanian, K. S., & Aruldoss, J. A. (1999). Arsenic in drinking water—problems and solutions. *Water Science and Technology.* doi:10.1016/S0273-1223(99)00432-1.

Wan, J., Tang, G., & Qian, Y. (2007). Room temperature synthesis of single-crystal Fe_3O_4 nanoparticles with superparamagnetic property. *Applied Physics A: Materials Science and Processing.* doi:10.1007/s00339-006-3766-y.

Wang, J., Xu, W., Chen, L., Huang, X., & Liu, J. (2014). Preparation and evaluation of magnetic nanoparticles impregnated chitosan beads for arsenic removal from water. *Chemical Engineering Journal.* doi:10.1016/j.cej.2014.04.061.

Wang, Y., Wang, S., Wang, X., Zhang, Z., & Jia, Y. (2016). Adsorption behavior and removal mechanism of arsenic from water by Fe (III)-modified 13X molecular sieves. *Water, Air, & Soil Pollution.* doi:10.1007/s11270-016-2955-3.

Yavuz, C. T., Mayo, J. T., Yu, W. W., Prakash, A., Falkner, J. C., Yean, S., Cong, L., Shipley, H. J., Kan, A., Tomson, M., Natelson, D., & Colvin, V. L. Monodisperse low-field magnetic separation of Fe_3O_4 nanocrystals. *Science.* doi:10.1126/science.1131475.

Yean, S., Cong, L., Yavuz, C. T., Mayo, J. T., Yu, W. W., Kan, A. T., Colvin, V. L., & Tomson, M. B. (2005). Effect of magnetite particle size on adsorption and desorption of arsenite and arsenate. *Journal of Materials Research.* doi:10.1557/jmr.2005.0403.